Giant asymmetry of soft x-ray magnetic scattering between opposite circular polarizations near the Brewster angle

Dae-Eun Jeong and Sang-Koog Kim*

Research Center for Spin Dynamics & Spin-Wave Devices and Nanospinics Laboratory, Department of Materials Science and Engineering, College of Engineering, Seoul National University, Seoul 151-744, Republic of Korea

(Received 26 May 2008; published 23 July 2008)

Giant asymmetry in soft x-ray resonant reflectivities of left- and right-handed circular polarization modes of an incident *p*-polarized beam from 3*d* transition-metal films was studied using newly developed theoretical and numerical calculations of soft x-ray resonant magnetic scattering based on *the circular-polarization-mode basis*. The physical origin of this novel phenomenon is completely destructive interference effect of soft x rays scattered individually from charge, orbital, and spin degrees of freedom in the resonant and nonresonant scattering. This destructive interference selectively occurs only for one circular mode of the two opposite circular polarizations under specific conditions of the energy and the incidence angle of soft x rays.

DOI: 10.1103/PhysRevB.78.012412 PACS number(s): 78.70.Ck, 78.20.Ls

Soft or hard x-ray resonant magnetic scattering (XRMS) has been widely used to probe and study charge, orbital, and spin degrees of freedom in multicomponent, ordered magnetic materials because it offers exceedingly enhanced, element-specific sensitivity to such different scattering sources interacting with incident x rays of energies close to the absorption edges of elements.[1–6] Due to a rich variety of microscopic interactions between incident photons and each of those scattering sources, as well as their angular and polarization dependences in the XRMS, the initial polarization state of incident photons can be converted to the different polarization states of the scattered photons with their angular variations,[1] in turn making it possible to determine element-specific charge, orbital, and spin orderings by analyzing the changes of the angular dependent polarization states of the scattered soft x rays.[5]

The right- and left-handed circular polarizations (RCP and LCP) are not only the basis of an irreducible representation of rotational symmetries in atomic transition processes,[7] but are also the eigenmodes of their interaction with the different kinds of orderings in broken symmetries, such as an ordered magnetic system.[8] Thus, the physical interpretation of the XRMS using the *circular-polarization-mode basis* is much more informative than the previously implemented *linear-polarization-mode basis* to the fundamental understanding of interactions between photons and various scattering sources as well as their essential polarization and angular dependences.

In this Brief Report, we report on the first observation of giant asymmetry in soft x-ray resonant reflectivities of the circular polarization components of incident *p*-polarized x rays from magnetic 3*d* transition-metal thin film, in proximity to the normal Brewster angle $\phi_B^n \cong 45°$. This phenomenon is found to be caused by a totally destructive interference occurring selectively for either circular polarization mode of photons scattered individually from charge, orbital, and spin degrees of freedom. This work is studied not only by the theoretical derivation of the XRMS amplitudes and phases of individual scattering sources using *the circular-polarization-mode basis* newly developed from this work, but also by the numerical calculations of the individual intensities of the RCP and LCP components using *the circular-mode-based magneto-optical Kerr matrices*.[9] Also, continuously variable polarization state, from the RCP, through the linear *s* polarization, to the LCP (or vice versa) is observed in a wide-angle region around ϕ_B^n.

First, we derive XRMS amplitudes with respect to the circular-mode basis by considering a total coherent elastic-scattering amplitude in the pure electric dipole ($E1$) transition for the case of 3*d* transition-metal ferromagnetic materials. The amplitude can be expressed by $f_{\text{tot}}=f_c+f_{\text{xres}}+f_m$, where f_c, f_m, and f_{xres} are the charge, nonresonant magnetic, and resonant scattering contributions, respectively.[10–12] In general, f_m is noticeably weaker than f_c by a factor of $\hbar\omega/mc^2 \simeq 0.002$ at $\hbar\omega=1$ keV, but f_{xres} is comparable to f_c and is much greater than f_m in the vicinity of the resonance edges.[10] Here, f_{xres} consists of the radial and angular parts. The former is represented by a reduced resonance scattering amplitude, $R'(l_1,j_1;1;l_2)=\bar{R}(l_1,j_1;1;l_2)/\{1-[\Delta/\Gamma(x-i)]^2\}$ in a fast collision approximation and the latter by a *k*th rank spin-orbital coupled moment, $M^{(k)}(l_1,j_1;1;l_2)$, and the polarization tensor, $T^{(k)}(\hat{e}_r^*,\hat{k}_r;\hat{e}_i,\hat{k}_i)$, where $\hat{e}_{r(i)}$ and $\hat{k}_{r(i)}$ represent the polarization and propagation unit vectors of a reflected (incident) beam, respectively.[12]

The resonant scattering amplitudes with respect to the circular-mode basis are given in a matrix form by

$$\begin{aligned}\begin{pmatrix} f_{\text{xres}}^R \\ f_{\text{xres}}^L \end{pmatrix} &= 4\pi\lambda R'(l_1,j_1;1;l_2)\sum_{k=0}^{2}\sum_{q=-k}^{k}\sqrt{\frac{3}{2k+1}} \\ &\quad\times T_q^{(k)*}(\hat{e}_r^*,\hat{k}_r;\hat{e}_i,\hat{k}_i)M_q^{(k)}(l_1,j_1;1;l_2) \\ &\simeq \frac{3}{2}\lambda R'(l_1,j_1;1;l_2)\Big[M^{(0)}(l_1,j_1;1;l_2)\mathbf{A} \\ &\quad -\frac{i}{\sqrt{2}}M_m^{(1)}(l_1,j_1;1;l_2)\mathbf{B}\Big]\begin{pmatrix} N_i^R \\ N_i^L \end{pmatrix}, \end{aligned} \tag{1}$$

where $M_m^{(1)}=M^{(1)}\cdot\hat{m}$ with a unit vector of magnetization, $\hat{m}=m_1\hat{u}_1+m_2\hat{u}_2+m_3\hat{u}_3$ and $N_i^{R(L)}$ implies the complex amplitude factor of the RCP (LCP) component with respect to the

circular-mode basis, $\hat{e}_i = N_i^R \hat{e}_i^R + N_i^L \hat{e}_i^L$. Since the magnetic linear dichroism term $M^{(2)}$ in the magnitude of the scattering amplitude for $3d$ transition metals is negligible,[8,11–13] only the $M^{(0)}$ and $M^{(1)}$ terms are considered in determining the scattering amplitudes.[14] The matrices of **A** and **B** are given as $\mathbf{A} = (\hat{e}_r^* \cdot \hat{e}_i)_{RL} = \mathbf{U}_{RL}^{sp\dagger} (\hat{e}_r^* \cdot \hat{e}_i)_{sp} \mathbf{U}_{RL}^{sp}$ and $\mathbf{B} = (\hat{e}_r^* \times \hat{e}_i)_{RL} = [\mathbf{U}_{RL}^{sp\dagger} (\hat{e}_r^* \times \hat{e}_i)_{sp} \mathbf{U}_{RL}^{sp}]$. The unitary operation in the matrices transforms a linear to circular polarization basis or vice versa, which leads to

$$\mathbf{A} = \begin{pmatrix} \frac{1}{2}(1+\cos 2\phi) & \frac{1}{2}(1-\cos 2\phi) \\ \frac{1}{2}(1-\cos 2\phi) & \frac{1}{2}(1+\cos 2\phi) \end{pmatrix}$$

and

$$\mathbf{B} = \begin{pmatrix} -\frac{1}{2} m_1 \sin 2\phi - i m_2 \cos\phi & \frac{1}{2} m_1 \sin 2\phi - i m_3 \sin\phi \\ \frac{1}{2} m_1 \sin 2\phi + i m_3 \sin\phi & -\frac{1}{2} m_1 \sin 2\phi + i m_2 \cos\phi \end{pmatrix},$$

where ϕ is the angle of incidence from a reflection surface as defined in Fig. 1. These matrices represent the polarization dependence of the total amplitude according to a given scattering geometry. The **A** is symmetric, independently of $\hat{m}$ and hence gives rise to its symmetric contribution to the scattering amplitude of each circular polarization. In contrast, the **B** is asymmetric with respect to the longitudinal and polar magnetizations. This originates from the conservation of each helicity in the presence of an axial symmetry with respect to $\hat{m}$.[7] For the longitudinal ($m_2 = \pm 1, m_1 = m_3 = 0$) and polar ($m_3 = \pm 1, m_1 = m_2 = 0$) magnetization cases, the **B** have the forms of

$$\mathbf{B}_{\mathbf{lon}} = \begin{pmatrix} -i m_2 \cos\phi & 0 \\ 0 & i m_2 \cos\phi \end{pmatrix}$$

and

$$\mathbf{B}_{\mathbf{pol}} = \begin{pmatrix} 0 & -i m_3 \sin\phi \\ i m_3 \sin\phi & 0 \end{pmatrix}.$$

The operation of **B** thus leads to $\hat{e}_i^{R(L)} \rightarrow \hat{e}_r^{R(L)}$ and $\hat{e}_i^{R(L)} \rightarrow \hat{e}_r^{L(R)}$ for each case, respectively, resulting in a possible asymmetric interference of scattered beams of the individual circular polarizations.

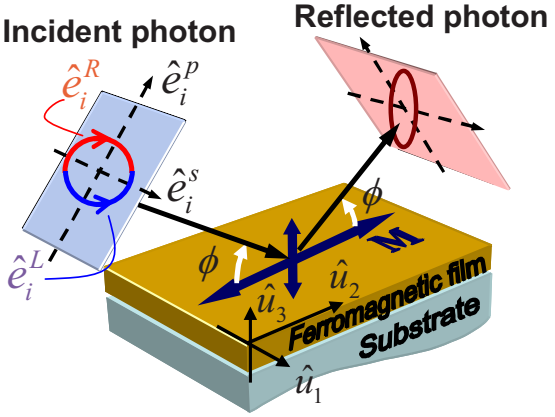

FIG. 1. (Color online) Definition and coordinate system used in the text for a specular reflection geometry with the linear s- and p- as well as RCP- and LCP-mode bases of the incident and reflected photons.

For the specific case of $E1$ resonant scattering at the line L_3 with $\hat{m} = +\hat{u}_2$, using the results of $\frac{3}{2}\chi R' \simeq \frac{2}{5}(e/\chi)^2 \{[(1 - (\Delta/\Gamma(x-i))^2)^{-1} |\langle 3d|r|2p_{3/2}\rangle|^2]/[\varepsilon_I - \varepsilon_b - \hbar\omega - i\Gamma/2]\} \equiv \frac{9}{2} iF$, $M^{(0)} \simeq \frac{2}{9}[N_h(2) - 2\Delta S_m/\Gamma(x-i)] \equiv \frac{2}{9}\bar{M}^{(0)}$, $M_m^{(1)} \simeq -\frac{1}{9\sqrt{2}}[S_m + 3L_m - \Delta N_h(2)/2\Gamma(x-i)] \equiv -\frac{1}{9\sqrt{2}}\bar{M}^{(1)}$, $f_{\mathrm{tot}}^{R,L}$ are finally obtained as

$$\begin{aligned} \begin{pmatrix} f_{\mathrm{tot}}^R \\ f_{\mathrm{tot}}^L \end{pmatrix} &= \left\{ [-r_0 F_c(\vec{K}) + iF\bar{M}^{(0)}]\mathbf{A} - \frac{F\bar{M}^{(1)}}{4}\mathbf{B} \right\} \begin{pmatrix} N_i^R \\ N_i^L \end{pmatrix} \\ &= \frac{1}{2}\left\{ -r_0 F_c(\vec{K}) + F\left[iN_h(2) + \frac{2\Delta S_m}{\Gamma} \right] \right\} \\ &\quad \times \begin{bmatrix} (N_i^R + N_i^L) + (N_i^R - N_i^L)\cos 2\phi \\ (N_i^R + N_i^L) - (N_i^R - N_i^L)\cos 2\phi \end{bmatrix} \\ &\quad + \frac{F}{4}\left[i(S_m + 3L_m) + \frac{\Delta N_h(2)}{2\Gamma} \right] \begin{pmatrix} m_2 \cos\phi N_i^R \\ -m_2 \cos\phi N_i^L \end{pmatrix}. \end{aligned} \tag{2}$$

Equation (2) shows that each of the charge $r_0 F_c(\vec{K})$, resonant nonmagnetic $F\bar{M}^{(0)}$, and resonant magnetic $F\bar{M}^{(1)}$ scattering terms individually contributes to f_{tot}^R and f_{tot}^L. The asymmetric polarization dependence between the RCP and LCP components gives rise to the differential scattering amplitude, i.e., $f_{\mathrm{tot}}^R \neq f_{\mathrm{tot}}^L$. It suggests that the maximum value of $(N_i^R - N_i^L)$ can yield the largest difference between f_{tot}^R and f_{tot}^L. The incident p-polarized beam, $\hat{e}_i^p = -\frac{i}{\sqrt{2}}\hat{e}_i^R + \frac{i}{\sqrt{2}}\hat{e}_i^L$, which consists of the RCP and LCP components with π phase difference, is the case, and $f_{\mathrm{tot}}^{R,L}$ for this case is given by

$$\begin{aligned} \begin{pmatrix} f_{\mathrm{tot}}^R \\ f_{\mathrm{tot}}^L \end{pmatrix} &= \frac{1}{\sqrt{2}}\left\{ ir_0 F_c(\vec{K}) + F\left[N_h(2) - i\frac{2\Delta S_m}{\Gamma} \right] \right\} \begin{pmatrix} \cos 2\phi \\ -\cos 2\phi \end{pmatrix} \\ &\quad + \frac{F}{4\sqrt{2}}\left[(S_m + 3L_m) - i\frac{\Delta N_h(2)}{2\Gamma} \right] \begin{pmatrix} \cos\phi \\ \cos\phi \end{pmatrix}. \end{aligned} \tag{3}$$

Here, we denote that $f_{\mathrm{tot}}^{R(L)} = f_c^{R(L)} + f_{\mathrm{xres:0}}^{R(L)} + f_{\mathrm{xres:1}}^{R(L)}$, where f_c, $f_{\mathrm{xres:0}}$ and $f_{\mathrm{xres:1}}$ represent the charge, resonant nonmagnetic

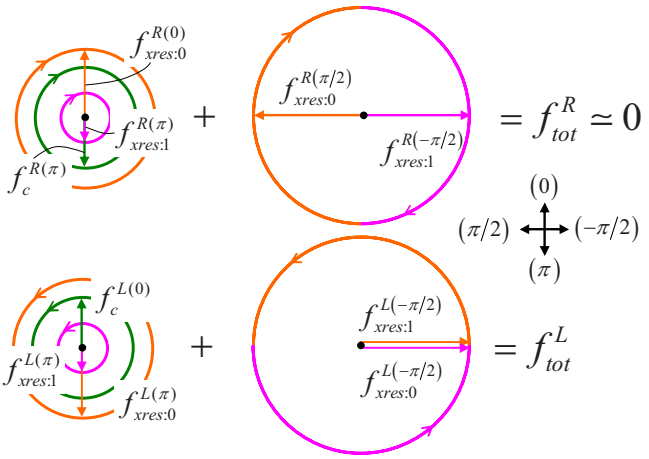

FIG. 2. (Color online) Illustration of interference effect in each of the RCP and LCP components of photons scattered individually from f_c, $f_{\mathrm{xres:0}}$, $f_{\mathrm{xres:1}}$ scattering sources, in terms of the real and imaginary terms. The radius of each circle represents the magnitude of the corresponding scattering amplitudes. The direction of the arrow inside each circle indicates the corresponding phase difference which is indicated in the parenthesis with respect to the incident p polarization.

and resonant magnetic scattering amplitudes, respectively. Due to the different angular dependences, i.e., $\cos 2\phi$ for $f_c^{R(L)}$ and $f_{\mathrm{xres:0}}^{R(L)}$, and $\cos\phi$ for $f_{\mathrm{xres:1}}^{R(L)}$, the magnitude of $f_{\mathrm{xres:1}}^{R(L)}$ could become comparable to $f_c^{R(L)}+f_{\mathrm{xres:0}}^{R(L)}$ at specific angles near ϕ_B^n. It can yield their differential reflectivities at some specific conditions, where either ($f_{\mathrm{tot}}^{R}\neq 0$, $f_{\mathrm{tot}}^{L}\cong 0$) or ($f_{\mathrm{tot}}^{L}\neq 0$, $f_{\mathrm{tot}}^{R}\cong 0$) can be fulfilled. A specific example for the case of $f_{\mathrm{tot}}^{L}\neq 0$ and $f_{\mathrm{tot}}^{R}\cong 0$ is illustrated in Fig. 2. We estimate the circular-polarization-selective Brewster angles $\phi_{B,+\mathrm{lon}}^{R(L)}$ by solving $f_{\mathrm{tot}}^{R(L)}=0$ at $\phi_{B,+\mathrm{lon}}^{R(L)}=45^\circ+\delta\phi_{B,+\mathrm{lon}}^{R(L)}$ for a strong resonant case of $r_0F_c<F$ in a first-order approximation of $\delta\phi_{B,+\mathrm{lon}}^{R(L)}$,

$$\delta\phi_{B,+\mathrm{lon}}^{R(L)} \cong +(-)\frac{\sqrt{2}(S_m+3L_m)}{16N_h(2)}-\left(\frac{S_m+3L_m}{16N_h(2)}\right)^2. \quad (4)$$

From Eq. (4), $\Delta\phi_{B,+\mathrm{lon}}=\phi_{B,+\mathrm{lon}}^{R}-\phi_{B,+\mathrm{lon}}^{L}$ is given approximately as $\sqrt{2}(S_m+3L_m)/8N_h(2)$. By inserting into Eq. (4) the numerical values of $F_c(\vec{K})\cong Z=28$, $F\cong 50r_0$, $S_m\cong 1.56$, $L_m\cong 0.13$, $N_h(2)\cong 2.5$, $\Gamma\cong 5$ eV, and $\Delta\cong 1.2$ eV for Co,[15–17] we estimate $\delta\phi_{B,+\mathrm{lon}}^{R(L)}=3.81^\circ(-4.09^\circ)$ and $\Delta\phi_{B,+\mathrm{lon}}=7.9^\circ$. These angular shifts from ϕ_B^n are quite large for the cases of $3d$-transition metals. This allows one to select either the LCP or RCP component of scattered soft x rays by changing the incidence angle across ϕ_B^n.

To verify the theoretical prediction of the giant asymmetric soft x-ray resonant reflectivities of the opposite photon helicities near ϕ_B^n, we also numerically calculated the intensities of the individual RCP and LCP components as well as the linear s and p components of photons reflected from a model of a 10-nm-thick Co layer on Si substrate, for both cases of $\hat{m}=\pm\hat{u}_2$ with a linearly p-polarized incident beam at the Co L_3 edge. In the calculations, we used the circular-mode-based magneto-optical Kerr matrix[10] and the optical

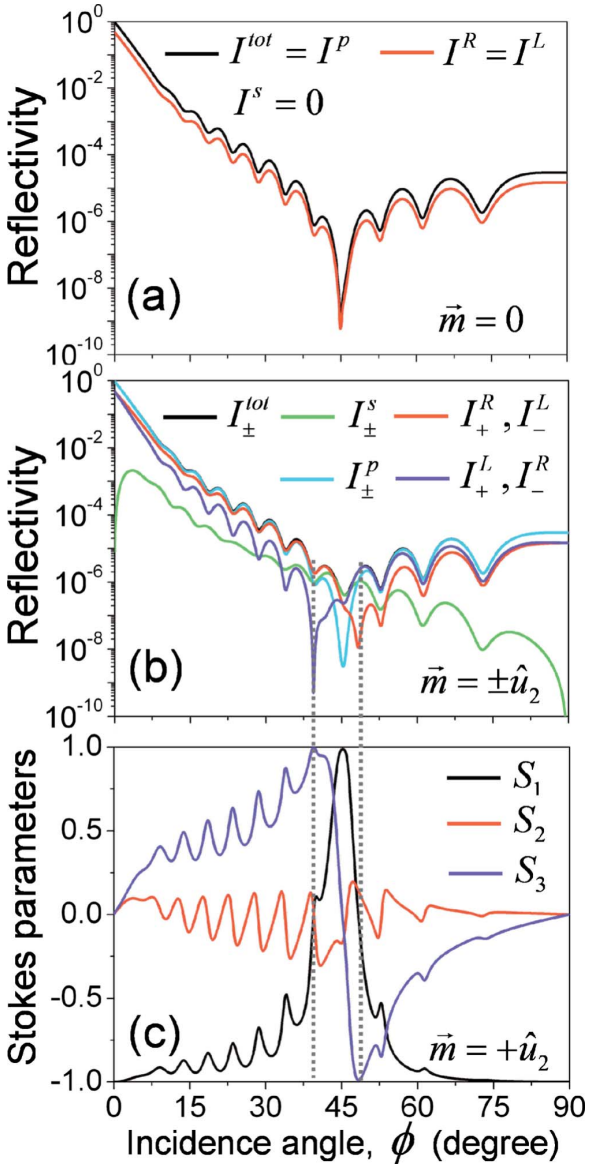

FIG. 3. (Color online) Calculations of the intensities of the linear s, p polarization and of the RCP and LCP at the Co L_3 edge for incident p-polarized x rays for (a) a demagnetization state of Co and (b) the longitudinally magnetized states of $\hat{m}=\pm\hat{u}_2$. The superscripts and subscripts in $I_{+,-}^{s,p,R,L}$ denote the corresponding polarization components in the scattered photons and either state of $\hat{m}=\pm\hat{u}_2$, respectively. (c) Calculations of the Stokes parameters as a function of ϕ for $\hat{m}=+\hat{u}_2$. The relations of the Stokes parameters and the degree of linear P_L or circular P_C polarization are expressed by $S_3=P_C$ and $S_1^2+S_2^2=P_L^2$.

parameters of a Co thin film obtained from soft x-ray circular dichroism spectra.[9] Figure 3(a) shows the angular variations of the individual reflectivities of individual polarization components for a demagnetized state of the Co film. In the reflectivity profiles, there exists only the ϕ_B^n due to no net magnetization. In comparison with the nonmagnetized case, contrasting reflectivity profiles between the individual polarization components are observed around ϕ_B^n from the longitudinally magnetized Co film for the incident p polarization, as shown in Fig. 3(b). As predicted by the XRMS theory

based on the circular-mode basis, the destructive interference of the LCP (RCP) component and the giant asymmetry in the reflectivities $\Delta I=(I_+^R-I_+^L)/I_+^L\cong 10^4$ and $(I_+^L-I_+^R)/I_+^R\cong 10^3$ are observed at $\phi_{B,+\mathrm{lon}}^L=39.5°$, $\phi_{B,+\mathrm{lon}}^R=48.4°$, respectively.

The degree of circular polarization, represented by the Stokes parameter S_3, thus reaches +1 or −1 at $\phi_{B,\pm\mathrm{lon}}^{R,L}$, indicating that almost pure circular polarizations can be obtained from the incident *p*-polarized beam and that the opposite photon helicities can be readily switchable either by changing the incident angle from $\phi_{B,\pm\mathrm{lon}}^L$ to $\phi_{B,\pm\mathrm{lon}}^R$ or simply by reversing the longitudinal magnetization, as seen from Fig. 3(c). Also, at $\phi_{B,\pm\mathrm{lon}}^p=45.2°$ the degree of linear polarization, represented by S_1, reaches +1, indicating the presence of the pure *s* polarization. The values of $\delta\phi_{B,+\mathrm{lon}}^{R(L)}=3.4°(-5.5°)$ obtained from the numerical calculations are in good agreement with $\delta\phi_{B,+\mathrm{lon}}^{R(L)}=3.81°(-4.09°)$ estimated from Eq. (4). In the above numerical calculations, it is worth noting that continuously variable polarization states can be obtained by changing ϕ across ϕ_B^n in a specular reflection geometry. The dramatic variation of the polarization state of scattered waves with the incidence angle can be described by maps of the Stokes parameters on the Poincaré sphere, as seen in Fig. 4. Reversing the magnetization direction yields the change of S_2 and S_3 in sign, and thus yields the switching between the opposite circular components. The variation from the RCP to LCP through the linear *s* polarization can be simply obtained by tuning ϕ to $\phi_{B,+\mathrm{lon}}^L=39.5°$, $\phi_{B,\pm\mathrm{lon}}^p=45.2°$, and $\phi_{B,+\mathrm{lon}}^R=48.4°$ in a wide angular range, or vice versa for the opposite magnetization orientation, as shown in Fig. 4.

In conclusion, we theoretically derived XRMS amplitudes for the individual RCP and LCP components of soft x rays scattered individually from the charge, orbital and spin degrees of freedom for a linearly *p*-polarized incident beam. From these derivations, we discovered giant asymmetric effect in soft x-ray resonant reflectivities of the opposite circular components in a wide incidence-angle range near ϕ_B^n.

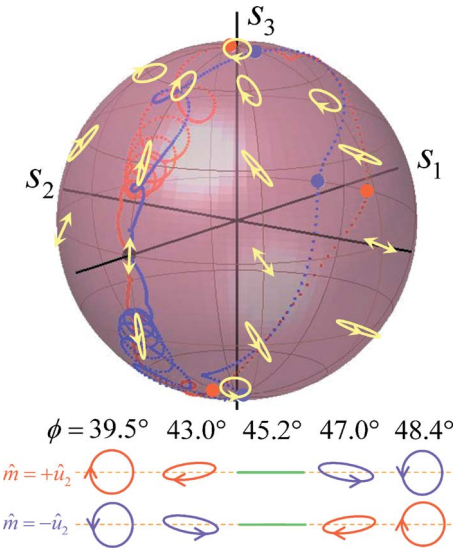

FIG. 4. (Color online) The mapping of the Stokes parameters on the Poincaré sphere as varying the incidence angle and continuously variable polarization states at the indicated angles in a wide angular region around ϕ_B^n, for $\hat{m}=+\hat{u}_2$ (red dotted line) and $\hat{m}=-\hat{u}_2$ (blue dotted line).

This novel phenomenon originates from totally destructive interference occurring selectively for either the RCP or LCP at specific angles in proximity to ϕ_B^n. Also, we found that there exist the opposite circular-mode-dependent Brewster angles in a wide angle range, as much as $\Delta\phi_{B,\mathrm{lon}}=8.9°$, and that the continuously variable polarization states are controllable with slight changes in the incident angle of a linearly *p*-polarized photon beam.

We express our thanks to J. B. Kortright for his careful reading of this manuscript. This work was supported by Creative Research Initiatives (ReC-SDSW) of MOST/KOSEF.

*Corresponding author. sangkoog@snu.ac.kr

[1] D. Gibbs, G. Grübel, D. R. Harshman, E. D. Isaacs, D. B. McWhan, D. Mills, and C. Vettier, Phys. Rev. B **43**, 5663 (1991).
[2] J. B. Kortright, D. D. Awschalom, J. Stöhr, S. D. Bader, Y. U. Idzerda, S. S. P. Parkin,Ivan K. Schuller, and H.-C. Siegmann, J. Magn. Magn. Mater. **207**, 7 (1999).
[3] J. B. Kortright, S.-K. Kim, G. P. Denbeaux, G. Zeltzer, K. Takano, and E. E. Fullerton, Phys. Rev. B **64**, 092401 (2001).
[4] L. Braicovich, G. Ghiringhelli, A. Tagliaferri, G. van der Laan, E. Annese, and N. B. Brookes, Phys. Rev. Lett. **95**, 267402 (2005).
[5] G. Srajer, L. H. Lewis, S. D. Bader, A. J. Epstein, C. S. Fadley, E. E. Fullerton, A. Hoffmann, J. B. Kortright, K. M. Krishnan, S. A. Majetich, T. S. Rahman, C. A. Ross, M. B. Salamon, I. K. Schuller, T. C. Schulthess, and J. Z. Sun, J. Magn. Magn. Mater. **307**, 1 (2006).
[6] O. Prokhnenko, R. Feyerherm, E. Dudzik, S. Landsgesell, N. Aliouane, L. C. Chapon, and D. N. Argyriou, Phys. Rev. Lett. **98**, 057206 (2007).
[7] V. B. Berestetskii, E. M. Lifshitz, and L. P. Pitaevskii, *Quantum Electrodynamics* (Pergamon, Oxford, 1982).
[8] P. Carra, B. T. Thole, M. Altarelli, and X. Wang, Phys. Rev. Lett. **70**, 694 (1993).
[9] D.-E. Jeong, K.-S. Lee, and S.-K. Kim, Appl. Phys. Lett. **88**, 181109 (2006).
[10] M. Blume, J. Appl. Phys. **57**, 3615 (1985).
[11] J. P. Hannon, G. T. Trammell, M. Blume, and D. Gibbs, Phys. Rev. Lett. **61**, 1245 (1988); **62**, 2644(E) (1989).
[12] J. Luo, G. T. Trammell, and J. P. Hannon, Phys. Rev. Lett. **71**, 287 (1993).
[13] G. van der Laan, Phys. Rev. Lett. **82**, 640 (1999).
[14] This is a case where the symmetry is with a magnetic ordering and a negligible crystal-field effect.
[15] C. Kao, J. B. Hastings, E. D. Johnson, D. P. Siddons, G. C. Smith, and G. A. Prinz, Phys. Rev. Lett. **65**, 373 (1990).
[16] R. Wu and A. J. Freeman, Phys. Rev. Lett. **73**, 1994 (1994).
[17] S.-K. Kim and J. B. Kortright, Phys. Rev. Lett. **86**, 1347 (2001).